Muscle-Specific Deletion of Rictor Impairs Insulin-Stimulated Glucose Transport and Enhances Basal Glycogen Synthase Activity[▽]

Anil Kumar,[1]* Thurl E. Harris,[1] Susanna R. Keller,[2] Kin M. Choi,[1]†
Mark A. Magnuson,[3] and John C. Lawrence, Jr.[1]‡

*Department of Pharmacology, University of Virginia Health System, Charlottesville, Virginia 22908[1]; Internal Medicine, Division of
Endocrinology, University of Virginia Health System, Charlottesville, Virginia 22908[2]; and Center for Stem Cell Biology and
Department of Molecular Physiology and Biophysics, Vanderbilt University Medical Center, Nashville, Tennessee 37232[3]*

Rictor is an essential component of mTOR (mammalian target of rapamycin) complex 2 (mTORC2), a kinase complex that phosphorylates Akt at Ser473 upon activation of phosphatidylinositol 3-kinase (PI-3 kinase). Since little is known about the role of either rictor or mTORC2 in PI-3 kinase-mediated physiological processes in adult animals, we generated muscle-specific rictor knockout mice. Muscle from male rictor knockout mice exhibited decreased insulin-stimulated glucose uptake, and the mice showed glucose intolerance. In muscle lacking rictor, the phosphorylation of Akt at Ser473 was reduced dramatically in response to insulin. Furthermore, insulin-stimulated phosphorylation of the Akt substrate AS160 at Thr642 was reduced in rictor knockout muscle, indicating a defect in insulin signaling to stimulate glucose transport. However, the phosphorylation of Akt at Thr308 was normal and sufficient to mediate the phosphorylation of glycogen synthase kinase 3 (GSK-3). Basal glycogen synthase activity in muscle lacking rictor was increased to that of insulin-stimulated controls. Consistent with this, we observed a decrease in basal levels of phosphorylated glycogen synthase at a GSK-3/protein phosphatase 1 (PP1)-regulated site in rictor knockout muscle. This change in glycogen synthase phosphorylation was associated with an increase in the catalytic activity of glycogen-associated PP1 but not increased GSK-3 inactivation. Thus, rictor in muscle tissue contributes to glucose homeostasis by positively regulating insulin-stimulated glucose uptake and negatively regulating basal glycogen synthase activity.

Insulin signaling is essential for glucose homeostasis. In muscle, insulin promotes both glucose uptake and the incorporation of glucose into glycogen, processes that contribute greatly to insulin-mediated glucose disposal after a meal (49). Defects in glucose uptake and glycogen synthesis, which occur in diabetes, are implicated in the development of hyperglycemia and, over time, in other complications (12). Both glucose transport (49) and glycogen synthase activation (31) are considered to be rate-limiting steps for glycogen synthesis in skeletal muscle. In myocytes, insulin signaling enhances glucose entry into the cell by translocating the glucose transporter GLUT4 from intracellular sites to the cell surface (27). In addition, insulin signaling enhances the incorporation of glucose into glycogen by activating glycogen synthase after inducing its dephosphorylation (38).

Many of the physiological processes regulated by insulin signaling are mediated by phosphatidylinositol 3-kinase signaling via the serine/threonine (Ser/Thr) kinase Akt (PKB) (54). Although the precise mechanisms by which insulin stimulates glucose uptake remain to be established, direct Akt substrates, like AS160 (25), may play an important role by regulating

GLUT4 translocation to the cell surface (21). Activation of glycogen synthase by insulin involves phosphorylation and inactivation of the α and β isoforms of the Akt substrate glycogen synthase kinase 3 (GSK-3) at Ser9 and Ser21, respectively (10). In the basal state, GSK-3 phosphorylates glycogen synthase at sites 3a, 3b, 3c, and 4, corresponding to Ser641, -645, -649, and -653 in the COOH terminus, and inactivates glycogen synthase (38, 39). Phosphorylated GSK-3 target sites in glycogen synthase are actively dephosphorylated in response to insulin by glycogen-associated protein phosphatase 1 (PP1) (35).

Insulin signaling rapidly activates Akt by phosphorylation at two residues, Thr308 and Ser473, both of which are required for full activation of this kinase in vitro (1, 3). Thr308, which resides in the activation loop of Akt, is phosphorylated by phosphoinositide-dependent kinase 1 (PDK1) (2). A previously unknown kinase, similarly termed PDK2, had been proposed to mediate the phosphorylation of Ser473 in the COOH-terminal hydrophobic motif of Akt. Recent studies have convincingly established that PDK2 is the mTOR (mammalian target of rapamycin) complex 2 (mTORC2) (20, 44).

mTOR is a Ser/Thr kinase that has long been known to regulate cell growth and proliferation in response to insulin, nutrients, and growth factors. Studies over the past few years have shown that mTOR is the catalytic subunit of at least two distinct multiprotein complexes (55). mTOR complex 1 (mTORC1), formed by mTOR interaction with raptor, mLST8 (55), and PRAS40 (53), phosphorylates S6K1 and 4EBP1 in response to insulin and growth factor stimulation and is sensitive to rapamycin inhibition (55). On the other hand, mTORC2, which is composed of rictor (rapamycin-insensitive

---

* Corresponding author. Mailing address: Department of Pharmacology, University of Virginia Health System, P.O. Box 800735, 1300 Jefferson Park Ave., Charlottesville, VA 22908. Phone: (434) 924-1582. Fax: (434) 982-3878. E-mail: al4p@virginia.edu.
† Present address: Primanova Biosciences, Inc., 3235 Route 112, Medford, NY 11763.
‡ Died on 19 December 2006.

companion of mTOR), mLST8, mSin1, and mTOR, is acutely insensitive to rapamycin (23, 55). Disruption of mTORC2 in mice by homozygous deletion of rictor (16, 48), mLST8 (16), or mSin1 (23) causes embryonic lethality. Therefore, the physiological role of mTORC2 could not be established. Studies using mouse embryonic fibroblasts (MEFs) that lack these genes have demonstrated that loss of mTORC2 eliminates Akt Ser473 phosphorylation. This results in the inhibition of insulin signaling to some, but not all, Akt substrates (16, 23, 48).

In this study we used mice containing a conditional rictor allele (Rictor$^{flox/flox}$) (48) to eliminate rictor in a muscle-specific manner. These mice were used to determine the role of mTORC2 in insulin-mediated glucose metabolism in the skeletal muscle of adult animals.

MATERIALS AND METHODS

Generation of MRic$^{-/-}$ mice. Rictor$^{flox/flox}$ mice (84.9% C57BL6/J, 15.1% 129S6) (48) were crossed with muscle creatine kinase (MCK)-Cre$^{+/-}$ transgenic mice (6) to obtain heterozygous MCK-Cre$^{+/-}$ Rictor$^{flox/WT}$ offsprings (where WT is wild type) in the F1 generation. These heterozygous mice were crossed with Rictor$^{flox/flox}$ mice to obtain the muscle-specific rictor knockout mice with genotype MCK-Cre$^{+/-}$ Rictor$^{flox/flox}$ (referred to in the paper as MRic$^{-/-}$ or knockout) in the F2 generation. The MRic$^{-/-}$ mice were then crossed with Rictor$^{flox/flox}$ mice to generate the MRic$^{-/-}$ mice and their MCK-Cre$^{+/-}$ Rictor$^{flox/flox}$ littermates (referred to in the paper as MRic$^{+/+}$ or wild type) in the F3 and following generations. Age-matched MRic$^{+/+}$ and MRic$^{-/-}$ mice of both sexes were studied at 3 to 5 months. For all mice used, the genotype was determined by PCR analysis of tail genomic DNA as described previously (6, 48). The mice were maintained under temperature- and humidity-controlled conditions with a 12-h light, 12-h dark cycle and were allowed food and water ad libitum. All animal studies performed in this investigation were approved by the University of Virginia Animal Care and Use Committee.

Reverse transcriptase PCR. Total RNA was extracted from fresh tissues (skeletal muscle and fat) by use of TRIzol reagent (Invitrogen), and cDNA was synthesized with a Qiagen Omniscript cDNA synthesis kit. PCR was performed using the forward primer 5′-GCGGCCGCTCTCTGAAGAACC-3′ and the reverse primer 5′-AGCCCATCATTTCCAACCGC-3′ to obtain a 510-bp product spanning bases 40 to 550 of the wild-type rictor cDNA (GenBank accession number AY540053 [48]).

In vivo insulin stimulation. After overnight fasting, mice were anesthetized by intraperitoneal injection of 0.1 ml/kg body weight of a mixture of ketamine (40 mg/ml), xylazine (10 mg/ml), and acepromazine (1.5 mg/ml) in saline. After 20 min, animals were given an intraperitoneal injection of saline or insulin (Novolin, 150 mU/g body weight [32]). Hind limb muscles were exposed, and after 15 min samples weighing ~50 mg were obtained by compressing part of the exposed muscles between metal tongs that were precooled in liquid nitrogen and excising the frozen tissue. The epididymal or parametrial fat pads were dissected and immediately dipped in liquid nitrogen. The frozen tissue samples were stored at −80°C until further processing. The frozen tissues were ground manually with a porcelain mortar and pestle that had been chilled in liquid nitrogen. The powdered muscles were used for immunoblotting, glycogen synthase activity assays, and membrane/glycogen pellet preparations. Adipose tissue samples were powdered and used for immunoblotting.

Incubation of muscles ex vivo. Krebs-Henseleit buffer (118 mM NaCl, 4.7 mM KCl, 2.5 mM CaCl$_2$, 1.2 mM potassium phosphate, 1.2 mM MgSO$_4$, 25 mM NaHCO$_3$ [pH 7.4]) was gassed continuously by bubbling with a mixture of 95% O$_2$ and 5% CO$_2$ for at least 30 min. Extensor digitalis longus (EDL) muscles were dissected from overnight-fasted mice and incubated at 37°C in the pregassed Krebs-Henseleit buffer (10 ml/muscle) containing 5 mM glucose for 45 min to remove endogenous hormones. The muscles were then incubated for 30 min without or with 100 mU/ml insulin at 37°C in the same buffer. To terminate the incubations, the muscles were blotted on tissue paper and immediately frozen in liquid nitrogen. The frozen muscles were powdered as described above, and protein extracts were prepared for immunoblotting and also for glycogen synthase activity assays.

Preparation of tissue extracts for immunoblotting and PP1 activity. The powdered muscles were homogenized on ice by use of a Teflon glass homogenizer in 1 ml of ice-cold buffer (20 mM Tris-HCl [pH 7.4], 20 mM NaCl, 1 mM EDTA, 20 mM β-glycerophosphate, 5 mM EGTA, 1 mM dithiothreitol, 1 mM

phenylmethylsulfonyl fluoride [PMSF], 2 μg/ml aprotinin, 1 μg/ml leupeptin [17]) containing 0.1% Tween 20 and were centrifuged at 1,000 × g for 20 min at 4°C to pellet insoluble material. The protein concentration of the supernatant was determined. For immunoblotting, muscle extract samples (containing 25 to 100 μg of total protein) were subjected to sodium dodecyl sulfate-polyacrylamide gel electrophoresis (SDS-PAGE) in 7.5% or 10% polyacrylamide gels before proteins were transferred electrophoretically to Immobilon membranes (Millipore). After incubation with different antibodies, the membranes were washed, and antibody binding was detected using alkaline phosphatase-conjugated secondary antibodies and Tropix reagent (PerkinElmer Life Sciences). Relative signal intensities of bands in immunoblots were determined by scanning laser densitometry of X-ray films or by use of a Fujifilm LAS 3000 charge-coupled-device camera system with ImageQuant software (Molecular Dynamics). The level of phosphorylation of a particular protein was obtained after correcting for differences in the total level of that protein.

For PP1 activity measurements, extracts were prepared in 50 mM Tris-HCl (pH 7.5) buffer containing 0.1 mM EDTA, 0.5 mM EGTA, 1% Triton X-100, 0.1 mM Na-tosyl-Lys-chloromethyl ketone · HCl (TLCK), 2 mM benzamidine, 0.5 mM PMSF, 50 mM β-mercaptoethanol, 4 nM okadaic acid, 10 μg/ml leupeptin, and 2% glycogen.

Measurements of glycogen synthase activity. Muscle extracts were prepared by homogenizing the powdered muscles on ice using a tissue grinder (Teflon glass) in 800 μl of homogenization buffer (50 mM Tris-HCl [pH 7.8], 100 mM NaF, 10 mM EDTA). The homogenates were centrifuged for 5 min at 10,000 × g, and the supernatants were retained for analyses. The protein content of the extracts was measured and adjusted to a concentration of 1 mg/ml by adding homogenization buffer. Glycogen synthase activity was measured by the method of Thomas et al. (52). Muscle extracts (30 μl) were added to solutions (60 μl) containing 50 mM Tris-HCl (pH 7.8), 10 mg/ml rabbit liver glycogen, 20 mM EDTA, 25 mM NaF, and 10 mM UDP-[1-^{14}C]glucose (0.07 μCi/60 μl; Amersham Pharmacia Biotech) and incubated without or with 10 mM glucose-6-phosphate (G-6P) at 30°C for 20 min. G-6P is an allosteric activator of glycogen synthase and can activate even highly phosphorylated and inactive glycogen synthase. It is therefore used to determine total glycogen synthase activity. The glycogen synthase activity ratio was determined by dividing the activity measured without added G-6P by the activity measured in the presence of 10 mM G-6P (total activity).

Determination of 2-deoxy-glucose uptake into muscles. 2-Deoxy-glucose uptake in EDL muscle isolated from male mice fasted overnight was measured by a method described previously (4). Briefly, EDL muscles were incubated at 37°C in Krebs-Henseleit buffer either without or with 20 mU/ml insulin for 15 min and then transferred to the same buffer (10 ml/muscle) containing 0.5 mM 2-deoxy-[1,2-^{3}H]glucose (1 μCi/ml) and 10 mM [1-^{14}C]mannitol (0.1 μCi/ml). After stimulation without and with insulin for 15 min, incubations were terminated by washing the muscles in Krebs-Henseleit buffer at 4°C and freezing them in liquid nitrogen. The muscles were weighed and lysed in 1 N HCl at 65°C for 30 min. The samples were centrifuged at 13,000 × g, and the supernatant was transferred to a fresh tube and neutralized with 1 N NaOH. The radioactivity in the sample was determined in a liquid scintillation counter, set for counting dual labels. The values presented (μmol/ml intracellular water/h) for glucose uptake were corrected for the extracellular space, which was estimated from the amount of [^{14}C]mannitol recovered in the lysed muscles.

Glycogen content determination. Total cellular glycogen content was determined by modification of a method described by Passonneau and Lauderdale (36). Muscles were weighed (20 to 30 mg) and homogenized in 10 volumes of 0.03 N HCl. The homogenates were placed into boiling water for 5 min. The extracts (5 μl and/or 10 μl) were incubated with or without 50 ng amyloglucosidase per sample in 100 μl of 0.2 M sodium acetate, pH 4.8, at room temperature for 3 h and vortexed regularly to avoid sedimentation. Samples were then incubated with an assay cocktail (0.1 mM Tris-HCl [pH 8.0], 0.3 mM ATP, 6 mM MgCl$_2$, 5 mM dithiothreitol, 60 μM NADP$^+$, 2.5 U/ml hexokinase, and 1 μg/ml G-6P dehydrogenase) for 30 min at room temperature. Changes in fluorescence, as a result of NADPH production, were determined using a fluorometer. Reaction blank values were determined as the fluorescence of samples before enzymatic treatment with amyloglucosidase.

Preparation of total membrane/glycogen pellet. Muscle samples were homogenized with a polytron homogenizer in a HEPES-EDTA-sucrose (HES) buffer containing 20 mM HEPES (pH 7.5 at 4°C), 5 mM EDTA, 250 mM sucrose, 4 nM okadaic acid, 1 mM Na$_3$VO$_4$, 2 μg/ml pepstatin, 1 mM PMSF, 10 μg/ml aprotinin, and 2 μg/ml leupeptin (19). For homogenization, a 1:10 ratio of muscle to homogenization buffer was used. The homogenate was centrifuged at 1,200 × g at 4°C for 15 min, the postnuclear supernatant was transferred to a fresh tube, and the pellet was discarded. The postnuclear supernatant was then centrifuged at 220,000 × g for 4.5 h at 4°C. The pellet containing the total membrane/

glycogen fraction was resuspended in HES buffer and used to determine the levels of GLUT1, GLUT4, R_{GL}, PP1α, PP1β, glycogen synthase, and phosphorylated glycogen synthase at its Ser641 residue by immunoblotting or used to measure the glycogen-associated PP1 activity.

Determination of PP1 activity. ^{32}P-labeled glycogen phosphorylase was prepared by a method described by Cohen et al. (9). Muscle extracts or glycogen pellets (3 μg protein/reaction) prepared by the method described above were pretreated with 4 nM of okadaic acid for 2 min at 30°C in PP1 assay buffer containing 50 mM Tris-HCl (pH 7.5), 0.1 mM EDTA, and 25 mM β-mercaptoethanol. ^{32}P-labeled glycogen phosphorylase (15 μg/reaction) was incubated in PP1 assay buffer with 5 mM caffeine and 4 nM okadaic acid at 30°C for 5 min before being mixed with the okadaic acid-treated muscle extract. The mixture was incubated at 30°C for 10 min, and the level of phosphate released was determined by a method described previously (34).

Determination of GSK-3 activity. GSK-3 activity in the muscle extracts was determined using a muscle glycogen synthase peptide as described previously (40).

Intraperitoneal glucose/insulin tolerance tests. Mice were fasted overnight before intraperitoneal injection of 1 mg of glucose/g of body weight. The glucose solutions were prepared in 0.9% saline and warmed to 37°C for injections. Blood was sampled from the tail vein before (time zero) and 15, 30, 60, and 120 min after glucose injection. For insulin tolerance tests, random-fed animals were injected intraperitoneally with insulin (Novolin, 0.75 U/kg body weight) at about 2 pm. Blood glucose was sampled from the tail vein before injection (time zero) and 15, 30, 45, and 60 min after insulin injection. Blood glucose levels were determined using a glucometer (One Touch FastTake; LifeScan).

Miscellaneous. Nonesterified fatty acid levels were measured in serum obtained from overnight-fasted animals by using a NEFA-C kit from Wako Chemicals.

Animals, antibodies, and chemicals. The MCK-Cre transgenic mice were generously provided by C. Ronald Kahn (Joslin Diabetes Center). The anti-rictor antibody, the pan-actin antibody, and all phospho-specific antibodies except P-S641 GS and P-T642 AS160 were obtained from Cell Signaling Technology (Danvers, MA). The anti-GLUT1 antibody was obtained from Abcam (Cambridge, MA). The anti-R_{GL} antibody was generously provided by A. DePaoli-Roach (University of Indiana, Indianapolis). The P-S641 GS antibody was raised in rabbit by using the peptide corresponding to residues 635 to 644 of mouse muscle glycogen synthase with phosphorylated Ser641 (RYPRPVS$_P$VPP). The peptides used for raising the antibodies to glycogen synthase, GLUT4, PKBα, and mTOR have been described previously (29, 30, 45, 46). Total S6K1 antibody was raised in rabbit by using the peptide corresponding to residues 509 to 525 of mouse S6K1 (QAFPMISKRPEHLRMNL). Total GSK-3α antibody was raised in rabbit by using the peptide corresponding to residues 462 to 481 of rat GSK-3α (TETQTGQDWQAPDATPTLTN). PP1α and P-T642 AS160 antibody were obtained from Novus Biologicals (Littleton, CO). Phosphorylase kinase was purchased from Sigma Chemicals (St. Louis, MO). Total AS160 antibody, PP1β, and muscle glycogen synthase peptide were purchased from Upstate Biotechnology (Charlottesville, VA).

Statistics. Values shown are means ± standard errors (SE) for the numbers of animals indicated in the figure legends. Significance was determined by unpaired two-tailed t tests. Differences were considered significant if the P value was <0.05.

RESULTS

Muscle-specific deletion of rictor in mice. Mice with a muscle-specific deletion of rictor (MRic$^{-/-}$ mice) were obtained by crossing Rictor$^{flox/flox}$ and MCK-Cre transgenic mice. MCK-Cre-mediated excision of the floxed exon 3 (97 bp) in the *rictor* gene results in a tissue-specific deletion of rictor, as verified by analyzing RNA from hind limb muscles of MRic$^{+/+}$ and MRic$^{-/-}$ mice, respectively (Fig. 1A, lanes 2 and 3). RNA isolated from muscle of MRic$^{-/-}$ mice showed a 413-bp (Fig. 1A, lane 3) product, whereas a 510-bp product was seen by using muscle from MRic$^{+/+}$ mice (Fig. 1A, lane 2). The detection of only a 510-bp product in adipose tissue RNA of both MRic$^{+/+}$ and MRic$^{-/-}$ mice demonstrates the specificity of MCK-Cre-mediated gene deletion (Fig. 1A, lanes 4 and 5). To confirm that the frameshift in the rictor mRNA eliminates protein expression, MRic$^{-/-}$ mice extracts from both hind limb muscle and adipose tissue were
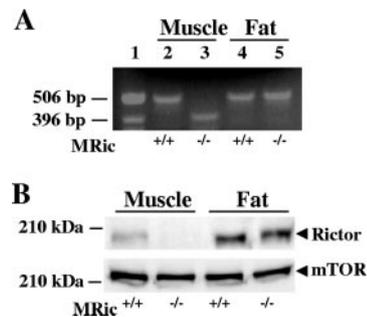
FIG. 1. Analysis of rictor gene expression in MRic$^{-/-}$ mice. (A) Total RNA extracted from skeletal muscle (muscle) and adipose tissue (fat) was analyzed by reverse transcriptase PCR (lanes 2 to 5). A 1-kb DNA ladder (Invitrogen) was used as the molecular mass marker (lane 1). (B) Tissue extracts prepared from skeletal muscle and adipose tissue were subjected to SDS-PAGE and were immunoblotted with anti-rictor antibodies (top). The mTOR immunoblot shown in the bottom panel served as the loading control in these experiments.

immunoblotted with anti-rictor antibody (Fig. 1B, top). Rictor protein level was reduced by ~90% in muscle, whereas it was normal in adipose tissue, of MRic$^{-/-}$ mice. Thus, both RNA and protein analyses demonstrate the efficient and specific ablation of rictor gene expression in skeletal muscle of MRic$^{-/-}$ mice. The MRic$^{-/-}$ mice were born at the expected Mendelian ratio and did not display any apparent defects in fertility or maturation (data not shown).

Rictor ablation in muscle decreases in vivo insulin-stimulated phosphorylation of Akt Ser473 but not Thr308. mTORC2 phosphorylates Akt at Ser473, and this phosphorylation has been proposed to determine phosphorylation at Thr308 (44). To evaluate whether rictor plays a role in Akt Ser473 and Thr308 phosphorylation in vivo, hind limb muscle extracts prepared from saline- (basal) and insulin-injected MRic$^{+/+}$ and MRic$^{-/-}$ mice were immunoblotted with phospho-Ser473 and phospho-Thr308 Akt antibodies. Insulin caused a 10- to 15-fold increase in the phosphorylation of Akt at Ser473 in MRic$^{+/+}$ muscles (Fig. 2A and B) compared to the level in muscles from saline-injected MRic$^{+/+}$ mice. However, in MRic$^{-/-}$ muscles, the insulin-stimulated increase in Akt Ser473 phosphorylation was less than twofold, corresponding to an approximately 85% reduction in the level of Ser473-phosphorylated Akt compared to the level in insulin-injected MRic$^{+/+}$ muscles (Fig. 2A and B). Interestingly, in MRic$^{-/-}$ muscles Akt was phosphorylated at Thr308 (Fig. 2A and C). Phosphorylation at this site in Akt was even slightly increased in saline-injected MRic$^{-/-}$ mice (~2-fold) compared to the level in saline-injected MRic$^{+/+}$ mice (Fig. 2A and C). The insulin-treated MRic$^{-/-}$ mice showed Akt Thr308 phosphorylation similar to that of the MRic$^{+/+}$ mice. However, due to increased basal phosphorylation, phosphorylated Akt Thr308 was increased only approximately 2.5-fold over the basal level in MRic$^{-/-}$ muscles, compared to a fivefold increase over the basal level in insulin-stimulated MRic$^{+/+}$ muscles (Fig. 2A and C). The same extracts showed similar levels of expression of Akt in muscles of both genotypes (Fig. 2A).

To determine whether the impaired Akt Ser473 phosphorylation in MRic$^{-/-}$ muscles affects insulin signaling downstream of Akt, we assessed phosphorylation of Thr389 in S6K1, a target of
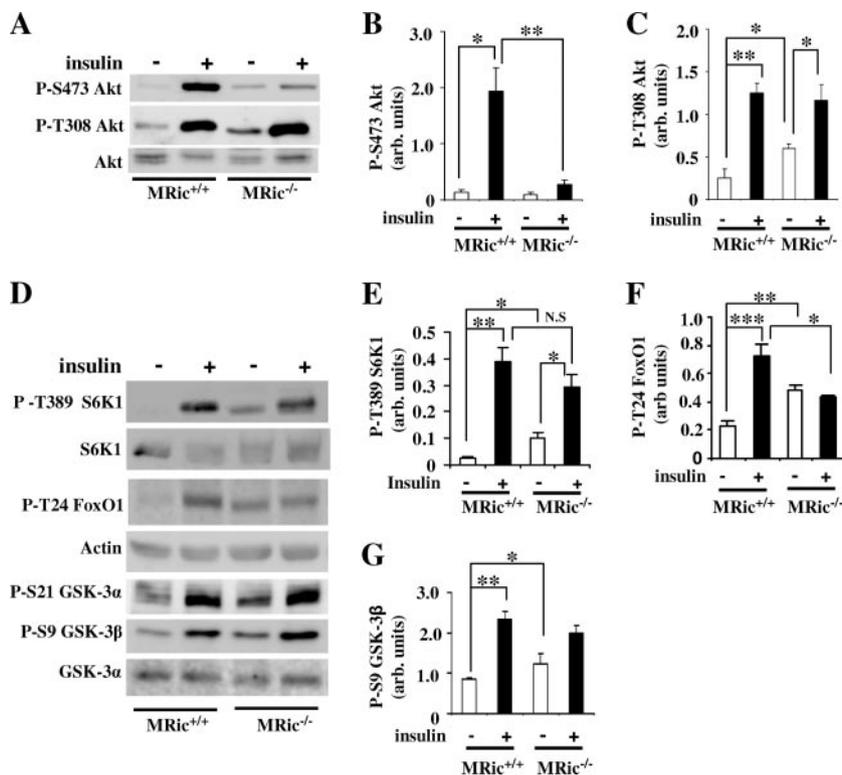
FIG. 2. In vivo insulin-stimulated phosphorylation of Akt at Ser473 was abolished but phosphorylation of Akt at Thr308 was normal in MRic$^{-/-}$ muscles. (A) Muscle extracts (25 to 100 μg total protein) prepared from mice intraperitoneally injected with saline (−) or insulin (+) were subjected to SDS-PAGE and immunoblotted with phospho-specific antibodies to sites in Akt (P-S473 and P-T308 [P-S, phospho-Ser; P-T, phospho-Thr]) and total Akt antibody. The quantification data (means ± SE) presented are for immunoblots of (B) P-S473 Akt ($n = 5$ per group; ∗, $P < 0.03$; ∗∗, $P < 0.002$) and (C) P-T308 Akt ($n = 4$ per group; ∗, $P < 0.04$; ∗∗, $P < 0.0006$). (D) Protein extracts from muscle were immunoblotted with phospho-specific antibodies to S6K1 (P-T389), FoxO1 (P-T24), and GSK-3 α/β (P-S21/9) as well as with antibodies to total S6K1, actin, and GSK-3α. (E to G) Data shown (means ± SE) reflect band intensity after normalization to the total detected protein or to the level of actin for (E) P-T389 S6K1 ($n = 4$; ∗, $P < 0.01$; ∗∗, $P < 0.0007$; N.S [not significant], $P < 0.2$), (F) P-T24 FoxO1 ($n = 5$; ∗, $P < 0.01$; ∗∗, $P < 0.0009$; ∗∗∗, $P < 0.0002$), and (G) P-S9 GSK-3β ($n = 4$; ∗, $P < 0.003$; ∗∗, $P < 0.001$). arb. units, arbitrary units.

mTORC1. While significantly increased in saline-injected MRic$^{-/-}$ mice, the levels of phosphorylation of S6K1 Thr389 were similar in insulin-treated MRic$^{+/+}$ and MRic$^{-/-}$ mice (Fig. 2D and E), and the total amount of S6K1 was unchanged in MRic$^{-/-}$ mice (Fig. 2D). Moreover, Akt-mediated FoxO1 phosphorylation at Thr24 was reduced in rictor knockout MEFs (16). In saline-injected MRic$^{-/-}$ muscle, FoxO1 Thr24 phosphorylation was increased compared to the level in saline-injected MRic$^{+/+}$ mice (Fig. 2D and F). Insulin treatment did not further induce FoxO1 phosphorylation in MRic$^{-/-}$ muscles but caused about a threefold increase in MRic$^{+/+}$ muscles (Fig. 2D and F).

Since insulin is known to stimulate phosphorylation of Akt substrates GSK-3 α and β at Ser21 and Ser9 residues (10), we tested whether this response was impaired in muscles from MRic$^{-/-}$ mice. Compared to levels in muscles obtained from saline-injected MRic$^{+/+}$ mice, the phosphorylation levels of both Ser21 and Ser9 in GSK-3 α and β were increased 1.5- to 2-fold in muscles from saline-injected MRic$^{-/-}$ mice (Fig. 2D and G), and insulin treatment increased the phosphorylation at both of these residues in GSK-3 α and β to similar extents in the muscle extracts of MRic$^{+/+}$ and MRic$^{-/-}$ mice (Fig. 2D and G).

Basal glycogen synthase activity is increased in MRic$^{-/-}$ muscles. To determine whether the loss of rictor in skeletal muscle affects glycogen synthesis, we measured the glycogen syn-

thase activity ratio in MRic$^{-/-}$ muscles. The glycogen synthase activity ratio in skeletal muscle extracts prepared from saline- and insulin-treated MRic$^{+/+}$ and MRic$^{-/-}$ mice is shown in Fig. 3A. In MRic$^{+/+}$ mice, the insulin-stimulated glycogen synthase activity ratio was increased ∼2-fold (0.168 ± 0.01 versus 0.088 ± 0.007, $n = 7$ per group, $P < 0.00003$), as previously reported (32, 47). Muscle from saline-injected MRic$^{-/-}$ mice showed a glycogen synthase activity ratio ∼80% higher than that of muscles from saline-injected wild-type animals (0.151 ± 0.017 in MRic$^{-/-}$ versus 0.088 ± 0.009 in MRic$^{+/+}$ mice, $n = 6$ to 7 per group, $P < 0.004$). Furthermore, insulin-stimulated glycogen synthase activity in MRic$^{-/-}$ muscles was similar to those in muscles from saline-injected MRic$^{-/-}$ and insulin-injected MRic$^{+/+}$ mice (0.148 ± 0.012 in insulin-injected versus 0.151 ± 0.017 in saline-injected MRic$^{-/-}$ mice, $n = 5$ to 6 per group). Using the same muscle extracts, we also assessed the phosphorylation of glycogen synthase at Ser641 (a site phosphorylated by GSK-3) and the total amount of glycogen synthase by immunoblotting with specific antibodies (Fig. 3B, top). It should be noted that the reduction in phosphorylation of glycogen synthase at Ser641 in muscle extracts from saline-injected MRic$^{-/-}$ mice is similar to that in MRic$^{+/+}$ mouse muscle after insulin treatment (Fig. 3B, bottom). The total amount of glycogen synthase in extracts from MRic$^{-/-}$ muscles was identical to that seen in MRic$^{+/+}$ muscles.
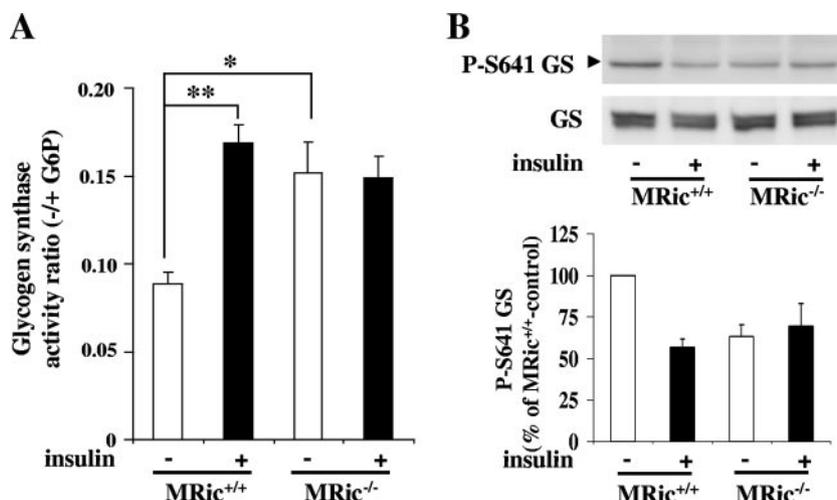
FIG. 3. Loss of rictor expression enhances basal glycogen synthase activity in muscle. (A) In vivo insulin-stimulated glycogen synthase activity in muscles of MRic$^{+/+}$ and MRic$^{-/-}$ mice. Glycogen synthase activity was measured using hind limb muscle extracts prepared from saline ($-$)- or insulin ($+$)-injected mice in the absence and presence of G-6P (10 mM). The activity ratios are the activity measured in the absence of G-6P divided by that in the presence of G-6P (total activity) (means $\pm$ SE, $n = 5$ to 7 per group; $*$, $P < 0.004$; $**$, $P < 0.00003$). (B) Muscle extracts used for the glycogen synthase assay were resolved by SDS-PAGE and immunoblotted with phospho-specific glycogen synthase (P-S641 GS) antibodies and total glycogen synthase (GS) antibodies (top). Quantification of P-S641 GS immunoblots is shown in the bottom panel ($n = 5$ per group).

When the same muscle extracts were tested for glycogen phosphorylase activity, no significant difference between the genotypes was detected (data not shown). Also, fasted MRic$^{+/+}$ and MRic$^{-/-}$ mice had similar muscle glycogen contents (3.50 ± 0.68 µmol of glucose/g tissue in MRic$^{+/+}$ mice versus 3.18 ± 1.18 µmol glucose/g tissue in MRic$^{-/-}$ mice, $n = 5$ per group).

Increased basal and insulin-stimulated glycogen synthase activity in ex vivo-incubated MRic$^{-/-}$ muscle. We next measured the glycogen synthase activity ratio in EDL muscle by incubation in the absence or presence of insulin ex vivo. Muscle from the MRic$^{-/-}$ mice showed a higher basal glycogen synthase activity than muscle from MRic$^{+/+}$ mice (Fig. 4A) (0.161 ± 0.011 versus 0.114 ± 0.010, $n = 4$ per group, $P < 0.025$). In contrast to results from the in vivo experiments, insulin-stimulated glycogen synthase activity was ~31% higher

in MRic$^{-/-}$ muscles than in MRic$^{+/+}$ muscles (0.235 ± 0.011 versus 0.176 ± 0.010, $n = 4$ per group, $P < 0.006$). Rapamycin had no effect on insulin-stimulated glycogen synthase activity in muscle from mice of either genotype. Since the MRic$^{-/-}$ muscle incubated in the presence of rapamycin was devoid of both mTORC1 and mTORC2 activities, we conclude that activation of glycogen synthase in response to insulin is independent of both mTOR complexes.

To further assess the phosphorylation state of insulin signaling proteins, we performed additional immunoblotting experiments using protein extracts made from muscles incubated ex vivo (Fig. 4B). While insulin again failed to stimulate Akt Ser473 phosphorylation in the MRic$^{-/-}$ muscles, unlike results from the in vivo experiments there was no increase in the basal phosphorylation of Akt at Thr308 (Fig. 4B) or GSK-3β at Ser9 (Fig. 4B and C). However, insulin treatment increased the
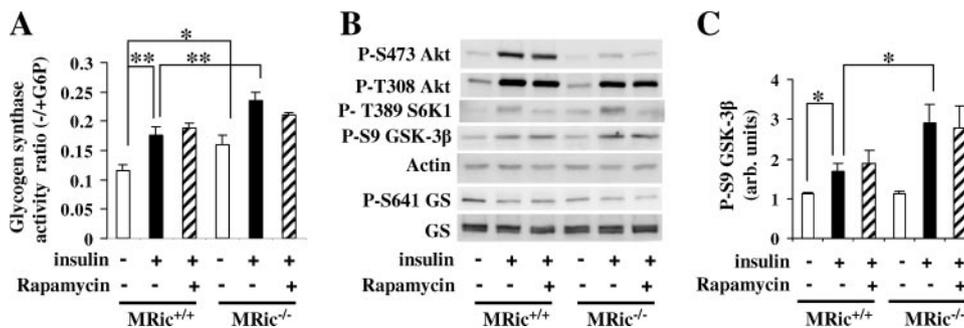
FIG. 4. Ex vivo-incubated MRic$^{-/-}$ muscle shows insulin-responsive glycogen synthase activity even with increased basal glycogen synthase activity. EDL muscles were incubated in Krebs-Henseleit buffer without ($-$) or with ($+$) insulin (100 mU/ml) for 30 min. The rapamycin-treated muscles were first incubated with rapamycin (200 nM final concentration) alone and then with rapamycin and insulin for 30 min. (A) Glycogen synthase activity was measured in EDL as described in the legend of Fig. 3A (means $\pm$ SE, $n = 4$ per group; $*$, $P < 0.025$; $**$, $P < 0.006$). (B) Protein extracts prepared from EDL muscles were subjected to SDS-PAGE and immunoblotted with phospho-specific antibodies to Akt, S6K1, GSK-3β, and glycogen synthase and antibodies to actin and total glycogen synthase. (C) Quantification of GSK-3β Ser9 phosphorylation (means $\pm$ SE, $n = 4$; $*$, $P < 0.01$) after normalization to actin. arb. units, arbitrary units.
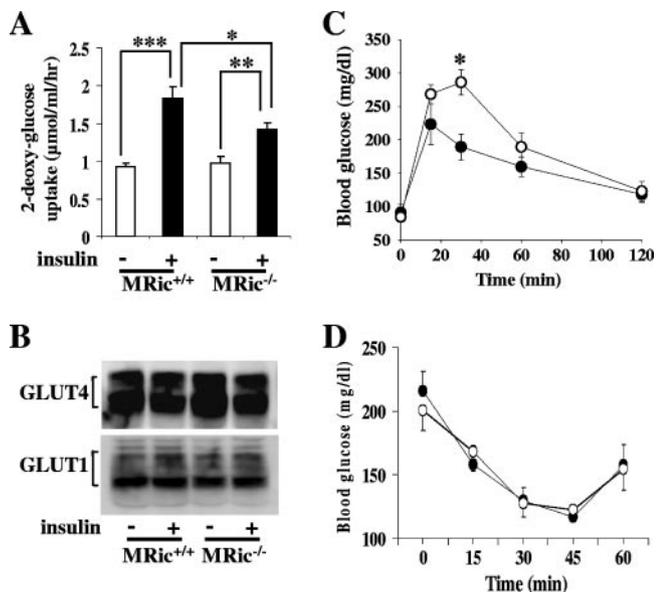
FIG. 5. Rictor ablation in muscle decreases insulin-stimulated glucose uptake, and MRic$^{-/-}$ mice exhibit impaired glucose tolerance. (A) EDL muscles were isolated and incubated with (+) or without (−) insulin (20 mU/ml) in medium containing 0.5 mM 2-deoxy-[1,2-^{3}H]glucose for 15 min. The results presented are means ± SE ($n = 4$ to 6; ∗, $P < 0.04$; ∗∗, $P < 0.007$; ∗∗∗, $P < 0.0005$). (B) Total membranes prepared from hind limb muscle homogenates of MRic$^{+/+}$ and MRic$^{-/-}$ mice were subjected to SDS-PAGE and immunoblotted with antibodies to GLUT4 and GLUT1 proteins. (C) Glucose tolerance tests were performed with six male MRic$^{+/+}$ (●) and seven male MRic$^{-/-}$ (○) mice. Blood glucose was measured at indicated times after an intraperitoneal injection of glucose (1 mg/g body weight) (∗, $P < 0.004$). (D) For insulin tolerance tests (male MRic$^{+/+}$ [●] and male MRic$^{-/-}$ [○] mice), blood glucose levels were measured in fed mice at indicated times after an intraperitoneal insulin injection (0.75U/kg body weight). The data presented are means ± SE of four to seven mice per group.

amount of GSK-3 phosphorylation 2.5-fold in MRic$^{-/-}$ muscles but only ~1.5-fold in wild-type muscles (Fig. 4B and C). The levels of phosphorylation of S6K1 at Thr389 in response to insulin were the same in MRic$^{-/-}$ and MRic$^{+/+}$ muscles, and phosphorylation was blocked by rapamycin in both genotypes. Rapamycin had no effect on insulin-stimulated GSK-3β Ser9 phosphorylation (Fig. 4B and C). Interestingly, a decrease in the basal phosphorylation of glycogen synthase at Ser641 was still observed for the ex vivo-incubated MRic$^{-/-}$ muscle, despite the presence of active GSK-3 as measured by Ser9 phosphorylation.

Decreased insulin-stimulated 2-deoxy-glucose uptake in EDL muscles and impaired glucose tolerance in male MRic$^{-/-}$ mice. Akt has been shown to be important for regulating insulin-mediated glucose transport (28). Moreover, it was possible that the observed increase in basal glycogen synthase activity (Fig. 3A and Fig. 4A) was due, at least in part, to increased basal transport of glucose and consequently increased levels of G-6P, an allosteric activator of glycogen synthase. For this reason we measured 2-deoxy-glucose uptake in EDL muscles isolated from male MRic$^{+/+}$ and MRic$^{-/-}$ mice (Fig. 5A). While levels of basal uptake were similar in MRic$^{+/+}$ muscles and MRic$^{-/-}$ muscles (0.925 ± 0.053 μmol/

ml/h, $n = 5$, versus 0.980 ± 0.075 μmol/ml/h, $n = 4$), insulin stimulation caused a twofold increase in glucose uptake in MRic$^{+/+}$ muscle (1.836 ± 0.158 μmol/ml/h, $n = 6$, $P < 0.0005$) but only 1.5-fold in MRic$^{-/-}$ muscle (1.429 ± 0.089 μmol/ml/h, $n = 6$, $P < 0.007$). This was an ~50% reduction in insulin-stimulated glucose uptake in MRic$^{-/-}$ muscles compared to MRic$^{+/+}$ muscles ($n = 6$, $P < 0.04$). The reduction in insulin-stimulated glucose uptake in muscles from MRic$^{-/-}$ mice could not be explained by changes in the levels of glucose transporters GLUT1 and GLUT4, as they were unaltered (Fig. 5B).

Since the lack of rictor in muscle causes both a reduction in insulin-stimulated glucose transport and an increase in basal glycogen synthase activity, we next sought to determine whether these defects are physiologically significant by performing intraperitoneal glucose tolerance tests with fasted male MRic$^{-/-}$ mice. The basal blood glucose concentration was the same in these animals as in the control mice (Fig. 5C). After a glucose bolus, the blood glucose concentrations were higher at 15, 30, and 60 min in MRic$^{-/-}$ mice; however, the observed difference in blood glucose concentrations of MRic$^{-/-}$ mice compared to those of wild-type mice was statistically significant only at 30 min (Fig. 5C) (189 ± 19 mg/dl in MRic$^{+/+}$ mice, $n = 6$, versus 285 ± 18 mg/dl in MRic$^{-/-}$ mice, $n = 7$; $P < 0.004$). Thus, in male MRic$^{-/-}$ mice the defects we observed in insulin signaling and glucose metabolism in muscle appear to cause impaired glucose tolerance. However, whole-body insulin sensitivity as measured by insulin tolerance test showed no significant difference (Fig. 5D). Serum nonesterified fatty acid levels were similar between MRic$^{+/+}$ and MRic$^{-/-}$ mice ($n = 10$ to 12 mice per group, 0.855 ± 0.08 meq/liter in MRic$^{+/+}$ mice and 0.810 ± 0.07 meq/liter in MRic$^{-/-}$ mice).

Defective insulin-stimulated AS160 Thr642 phosphorylation in MRic$^{-/-}$ muscles. Next, we tested the phosphorylation of AS160 at Thr642, a direct Akt substrate and a protein implicated in GLUT4 exocytosis (25). In the muscles of MRic$^{+/+}$ mice, there was an ~2-fold increase in AS160 Thr642 phosphorylation in response to insulin (Fig. 6). Although the AS160 phosphorylation at Thr642 was induced in muscles from insulin-treated MRic$^{-/-}$ mice, the increase was ~30% lower (1.7-fold) than in insulin-treated MRic$^{+/+}$ mice (Fig. 6). The defect in Akt-mediated AS160 phosphorylation could be partly responsible for the decreased insulin-stimulated glucose uptake in MRic$^{-/-}$ muscles.

Increased PP1 activity in glycogen pellets from MRic$^{-/-}$ muscles. To test whether PP1 plays a role in altered basal glycogen synthase activity in MRic$^{-/-}$ muscles, we next measured PP1 activity towards ^{32}P-labeled glycogen phosphorylase in whole muscle extracts and glycogen pellets. Previously, it was demonstrated that loss of insulin-stimulated glucose transport in muscles from muscle-specific GLUT4 knockout mice (57) leads to increased basal glycogen synthase activity (26), a condition similar to that found with MRic$^{-/-}$ muscles. In muscle-specific GLUT4 knockout muscles, there was an increase in total PP1 activity when measured in vitro using ^{32}P-labeled glycogen phosphorylase, due to upregulation in levels of R$_{GL}$, the muscle-specific regulatory subunit of PP1 (51), and another PP1 regulatory subunit, PTG. In contrast, in whole muscle extracts from MRic$^{-/-}$ mice, PP1 activity (Fig. 7A) as well as
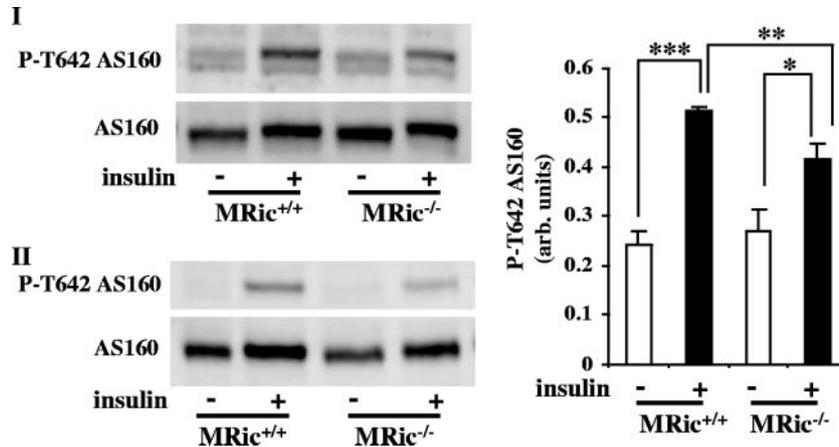
FIG. 6. AS160 Thr642 phosphorylation in MRic$^{-/-}$ muscle. Muscle extracts prepared from saline ($-$)- and insulin ($+$)-injected mice of both genotypes were subjected to SDS-PAGE and immunoblotted with phospho-specific antibody to Thr642 in AS160 and total AS160 antibody (I and II). Data (means $\pm$ SE) presented are the quantification of P-T642 AS160 immunoblots after normalizing for the level of total AS160 (right) ($n = 6$; *, $P < 0.025$; **, $P < 0.008$; ***, $P < 0.000001$). arb. units, arbitrary units.

total level of R_{GL} was unaltered (Fig. 7B). Among the four PP1 isoforms (α, β, $\gamma1$, and $\gamma2$), PP1α and PP1β are expressed in skeletal muscle (13). The levels of these PP1 isoforms were unchanged in whole muscle extracts from MRic$^{-/-}$ muscles (Fig. 7B). When measured in the muscle glycogen pellet, irrespective of whether the MRic$^{-/-}$ mice were injected with saline or insulin, PP1 activity was increased by 40 to 60% in the MRic$^{-/-}$ muscles compared to the level in MRic$^{+/+}$ muscles (Fig. 7C) (0.72 $\pm$ 0.03 nmol/10 min/mg protein versus 1.15 $\pm$ 0.07 nmol/10 min/mg protein in saline-treated MRic$^{+/+}$ and

MRic$^{-/-}$ mice, respectively, and 0.71 $\pm$ 0.12 nmol/10 min/mg protein versus 1.37 $\pm$ 0.12 nmol/10 min/mg protein in insulin-injected MRic$^{+/+}$ and MRic$^{-/-}$ mice, respectively; $n = 4$ to 5 per group; $P < 0.001$). Similarly to results seen with the whole muscle extracts (Fig. 3B), the levels of Ser641 phosphorylated glycogen synthase were decreased in the muscle glycogen pellets from saline-injected MRic$^{-/-}$ mice compared to levels in muscle glycogen pellets from saline-injected MRic$^{+/+}$ mice (Fig. 7D and E). The levels of glycogen synthase and R_{GL} were unaltered in the glycogen pellets compared between treat-
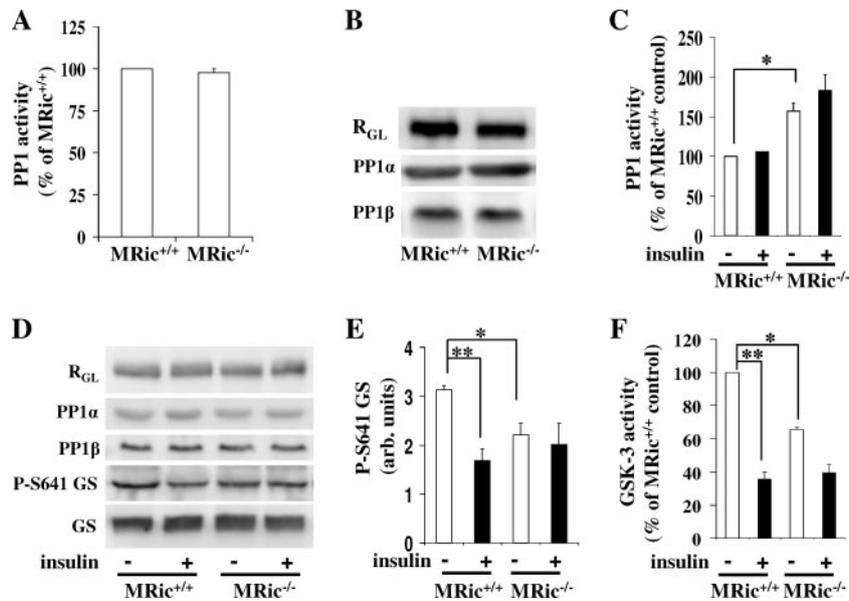
FIG. 7. Increased PP1 activity in muscle glycogen pellets from MRic$^{-/-}$ mice. PP1 activity in muscle extract (A) and glycogen pellet (C) from MRic$^{+/+}$ and MRic$^{-/-}$ mice, measured in the presence of 4 nM okadaic acid using ^{32}P-labeled glycogen phosphorylase as the substrate. (A) The muscle extracts (3 μg total protein) prepared from overnight-fasted mice were tested for PP1 activity. (B) The muscle extracts were immunoblotted for R_{GL}, PP1α, and PP1β. (C) PP1 activity determined in glycogen pellets prepared from muscles of MRic$^{+/+}$ and MRic$^{-/-}$ mice injected with saline ($-$) or insulin ($+$) (means $\pm$ SE, $n = 4$ to 5 mice per group; *, $P < 0.01$; **, $P < 0.005$). (D) Glycogen pellets were immunoblotted for R_{GL}, PP1α, PP1β, P-S641 GS, and GS. (E) Quantification of P-Ser641 GS immunoblots of glycogen pellet (means $\pm$ SE, $n = 4$ per group; *, $P < 0.01$; **, $P < 0.005$). arb. units, arbitrary units. (F) GSK-3 activity was measured in crude muscle extract in the absence and presence of 200 mM lithium chloride with a glycogen synthase peptide as the substrate (means $\pm$ SE, $n = 3$ per group; *, $P < 0.009$; **, $P < 0.0004$).

ments and genotypes (Fig. 7D). Similarly, the levels of PP1α and PP1β were the same in glycogen pellets of MRic$^{-/-}$ and MRic$^{+/+}$ muscles (Fig. 7D).

Last, we measured GSK-3 activity in muscle extracts from saline- or insulin-treated MRic$^{+/+}$ and MRic$^{-/-}$ mice (Fig. 7F). In MRic$^{+/+}$ mice, insulin caused an ~65% reduction in GSK-3 activity compared to activity in saline-injected mice of the same genotype (6.18 ± 0.32 pmol/min/mg protein versus 2.16 ± 0.18 pmol/min/mg protein; $n = 3$ per group; $P < 0.0004$). Consistent with the increase in the level of GSK-3 phosphorylated at Ser21/9 (Fig. 2D and G), the GSK-3 activity in saline-injected MRic$^{-/-}$ mice was reduced by ~35% compared to the activity in saline-injected MRic$^{+/+}$ mice (4.06 ± 0.29 pmol/min/mg protein versus 6.18 ± 0.18 pmol/min/mg protein; $n = 3$ per group; $P < 0.009$). Insulin-injected mice of both genotypes showed similar GSK-3 activities (2.16 ± 0.18 pmol/min/mg protein in MRic$^{+/+}$ mice and 2.4 ± 0.18 pmol/min/mg protein in MRic$^{-/-}$ mice; $n = 3$ per group).

DISCUSSION

We have used muscle-specific rictor knockout mice to show that the loss of rictor and presumably functional mTORC2 plays an important role in insulin signaling in muscle. In the absence of rictor, there is a dramatic decrease in Akt phosphorylation at Ser473 in response to insulin. Furthermore, skeletal muscle from MRic$^{-/-}$ mice exhibits both impaired insulin-mediated glucose uptake and increased glycogen synthase activity in the basal state. Our findings demonstrate that rictor, either as a component of mTORC2 or independently, is essential for the proper control of glucose uptake and the conversion of glucose into glycogen in skeletal muscle.

Since Akt activity is directly required for insulin-stimulated glucose uptake (8), it is possible that impaired Akt Ser473 phosphorylation affects the phosphorylation of a direct target of Akt that regulates redistribution of GLUT4 from intracellular sites to the cell surface (21, 56). In MRic$^{-/-}$ muscles, impaired phosphorylation of Akt Ser473 leads to diminished phosphorylation of AS160, an inhibitor of basal GLUT4 exocytosis (18). The Akt-mediated AS160 phosphorylation and consequent inhibition of Rab-GAP (GTPase activating protein) activity of AS160 have been proposed as a mechanism to increase insulin-mediated GLUT4 exocytosis (42). In addition, MRic$^{-/-}$ muscles could also have a defect in mTORC2-mediated regulation of the actin cytoskeleton (24, 43) contributing to reduced glucose uptake, as insulin-stimulated glucose uptake is an actin cytoskeleton-dependent process (18). Future experiments will examine exactly where the defect in insulin-stimulated glucose transport occurs in MRic$^{-/-}$ muscles.

In MRic$^{-/-}$ muscle, basal glycogen synthase activity is upregulated, reaching levels comparable to that of wild-type muscles after insulin stimulation. This effect can be mediated by increased expression of glycogen synthase, increased basal uptake of glucose, and changes in the phosphorylation state of glycogen synthase. Because there is no change in either total glycogen synthase levels or basal glucose uptake in MRic$^{-/-}$ muscles, it is unlikely that the observed increase in glycogen synthase activity occurs through increased expression or allosteric activation by G-6P. The phosphorylation of glycogen synthase at a GSK-3/PP1-regulated site (Ser641) was de-

creased in MRic$^{-/-}$ muscles under basal conditions. In vivo, this could be explained partly by decreased GSK-3 activity (Fig. 7F) caused by increased phosphorylation at the inhibitory site Ser21/9 in GSK-3 α/β (Fig. 2D and G). However, under ex vivo conditions the basal level of GSK-3 phosphorylation and presumably GSK-3 activity was unaltered (Fig. 4B and C). Interestingly, the basal activity and the phosphorylation of glycogen synthase showed a significant elevation and reduction, respectively, compared to levels for the wild type. This inconsistency suggested that a mechanism independent of GSK-3 might be responsible for the observed changes in basal glycogen synthase activity.

Further investigation into the increased basal activation of glycogen synthase led us to discover that PP1 activity was increased in glycogen pellets from MRic$^{-/-}$ muscles. The increased PP1 activity correlates with a decreased level of phosphorylated glycogen synthase and suggests that PP1-mediated dephosphorylation of glycogen synthase is responsible for the increase in basal glycogen synthase activity in MRic$^{-/-}$ muscle. The mechanism by which loss of rictor results in increased PP1 activity in muscle glycogen pellets is not known. In skeletal muscle, R$_{GL}$ (51) and PP1β (5) have been shown to be the most abundant glycogen targeting subunit and PP1 isoform, respectively. PP1β is also reported to be the major R$_{GL}$-associated PP1 isoform (7, 13). Loss of R$_{GL}$ expression in mice causes an ~70% reduction in basal glycogen synthase activity and an ~50% reduction in PP1 activity in skeletal muscle (13). PTG is the other known subunit targeting PP1 to glycogen in skeletal muscle. Heterozygous PTG knockout mice exhibit reduced basal glycogen synthase activity (11). We have been unsuccessful in detecting PTG in muscle extracts and glycogen pellet. Since the levels of PP1α and PP1β were not changed in the glycogen pellets from MRic$^{-/-}$ muscle, it is likely that yet-to-be-defined modifications of glycogen-associated PP1 lead to enhanced specific activity of the enzyme.

Despite impaired glucose transport and altered glycogen synthase activity in skeletal muscle, the MRic$^{-/-}$ mice displayed only a mild impairment in glucose tolerance (Fig. 5C). Such discrepancies have been observed with different mouse models in which insulin signaling proteins and enzymes of glucose metabolism had been deleted. For example, muscle-specific insulin receptor knockout mice (6) and mice with a whole-body knockout of glycogen synthase 1 (muscle-specific isoform) (37) have defects in muscle glucose transport and glycogen synthase activity, respectively, yet both are glucose tolerant. In these mice, compensatory responses in the liver have been proposed to maintain normal glucose homeostasis. Supporting this notion, the liver-specific insulin receptor knockout mice have impaired glucose tolerance due to a lack of control of hepatic glucose production by insulin (33).

Interestingly, we observed a modest increase in basal levels of Akt phosphorylation at Thr308 in MRic$^{-/-}$ muscles. There are several possible causes for increased basal Akt Thr308 phosphorylation. First, since the phosphorylation of Akt at Thr308 by PDK1 is a PI3P (phosphatidylinositol-3,4,5-triphosphate)-dependent process, the increased phosphorylation may simply reflect increased signaling due to PI3P levels in MRic$^{-/-}$ muscles. Second, both the contraction of rat skeletal muscle (41) and increased cyclic AMP are known to induce phosphorylation of Akt at Thr308 (15). Thus, MRic$^{-/-}$ mus-

cles may have an increased response to the contraction of myotubes or increased sensitivity to a circulating factor in fasted mice that induces cyclic AMP in muscles. Consistent with the increase in basal levels of Akt Thr308 phosphorylation, we also observed increased basal phosphorylation of GSK-3 and S6K1 in MRic$^{-/-}$ muscles. The phosphorylation of both Ser9 and Ser21 of GSK-3α/β has also been reported to be mediated by PKA in HEK293 cells and NIH 3T3 cells (14).

Although phosphorylation of Akt at Ser473 in response to insulin was abolished completely in MRic$^{-/-}$ muscles, there was no effect on insulin-stimulated Akt Thr308 phosphorylation. This is in agreement with previous observations for rictor null MEFs and embryos (48) but contradicts another report that Ser473 phosphorylation is a determinant of Thr308 phosphorylation (44). Diminished or absent Ser473 phosphorylation reduces Akt activity when measured in vitro (48). Previous work has shown that loss of Ser473 phosphorylation did not affect Akt signaling to some direct substrates, including TSC2 and GSK-3 (16, 48). Our study confirms these observations. TSC2 phosphorylation by Akt in response to insulin is required to activate mTORC1 (22). Since insulin-induced mTORC1 activation was normal, as indicated by unaltered S6K1 Thr389 phosphorylation, there did not appear to be a defect in Akt signaling to TSC2 in MRic$^{-/-}$ muscles. Also, Thr308 phosphorylation of Akt by PDK1 is sufficient for Akt signaling to GSK-3 in MRic$^{-/-}$ muscles. S6K1 can phosphorylate GSK-3 in vitro (50). However, in MRic$^{-/-}$ muscle, GSK-3 phosphorylation is independent of S6K1, since rapamycin did not inhibit it. At this time, the only targets known to be affected by the loss of Akt Ser473 phosphorylation are FoxO1 at Thr24 and FoxO3a at Thr32 (16, 23). In MRic$^{-/-}$ muscle, there was a defect in FoxO1 phosphorylation in response to insulin. In addition, our study demonstrates that insulin-mediated phosphorylation of AS160 at Thr642 in muscles is partly dependent on Akt Ser473 phosphorylation. These results confirm that Ser473 phosphorylation of Akt is required for its activity towards some but not all of its substrates.

In closing, these studies further confirm that rictor is a necessary component of mTORC2 and is required for insulin-stimulated Ser473 phosphorylation of Akt. In addition, we demonstrate an essential role for rictor in insulin signaling in skeletal muscle. Rictor appears to function principally as a positive regulator of glucose transport. However, our studies also indicate that, under basal conditions, rictor functions as a negative regulator of PP1 activity towards glycogen synthase.

REFERENCES

1. **Alessi, D. R., M. Andjelkovic, B. Caudwell, P. Cron, N. Morrice, P. Cohen, and B. A. Hemmings.** 1996. Mechanism of activation of protein kinase B by insulin and IGF-1. EMBO J. **15:**6541–6551.

2. **Alessi, D. R., S. R. James, C. P. Downes, A. B. Holmes, P. R. Gaffney, C. B. Reese, and P. Cohen.** 1997. Characterization of a 3-phosphoinositide-dependent protein kinase which phosphorylates and activates protein kinase Balpha. Curr. Biol. **7:**261–269.

3. **Andjelkovic, M., D. R. Alessi, R. Meier, A. Fernandez, N. J. Lamb, M. Frech, P. Cron, P. Cohen, J. M. Lucocq, and B. A. Hemmings.** 1997. Role of translocation in the activation and function of protein kinase B. J. Biol. Chem. **272:**31515–31524.

4. **Azpiazu, I., J. Manchester, A. V. Skurat, P. J. Roach, and J. C. Lawrence, Jr.** 2000. Control of glycogen synthesis is shared between glucose transport and glycogen synthase in skeletal muscle fibers. Am. J. Physiol. Endocrinol. Metab. **278:**E234–E243.

5. **Barker, H. M., N. D. Brewis, A. J. Street, N. K. Spurr, and P. T. Cohen.** 1994. Three genes for protein phosphatase 1 map to different human chromosomes: sequence, expression and gene localisation of protein serine/threonine phosphatase 1 beta (PPP1CB). Biochim. Biophys. Acta **1220:**212–218.

6. **Bruning, J. C., M. D. Michael, J. N. Winnay, T. Hayashi, D. Horsch, D. Accili, L. J. Goodyear, and C. R. Kahn.** 1998. A muscle-specific insulin receptor knockout exhibits features of the metabolic syndrome of NIDDM without altering glucose tolerance. Mol. Cell **2:**559–569.

7. **Carmody, L. C., P. A. Bauman, M. A. Bass, N. Mavila, A. A. DePaoli-Roach, and R. J. Colbran.** 2004. A protein phosphatase-1gamma1 isoform selectivity determinant in dendritic spine-associated neurabin. J. Biol. Chem. **279:**21714–21723.

8. **Cho, H., J. Mu, J. K. Kim, J. L. Thorvaldsen, Q. Chu, E. B. Crenshaw III, K. H. Kaestner, M. S. Bartolomei, G. I. Shulman, and M. J. Birnbaum.** 2001. Insulin resistance and a diabetes mellitus-like syndrome in mice lacking the protein kinase Akt2 (PKB beta). Science **292:**1728–1731.

9. **Cohen, P., S. Alemany, B. A. Hemmings, T. J. Resink, P. Stralfors, and H. Y. Tung.** 1988. Protein phosphatase-1 and protein phosphatase-2A from rabbit skeletal muscle. Methods Enzymol. **159:**390–408.

10. **Cross, D. A., D. R. Alessi, P. Cohen, M. Andjelkovich, and B. A. Hemmings.** 1995. Inhibition of glycogen synthase kinase-3 by insulin mediated by protein kinase B. Nature **378:**785–789.

11. **Crosson, S. M., A. Khan, J. Printen, J. E. Pessin, and A. R. Saltiel.** 2003. PTG gene deletion causes impaired glycogen synthesis and developmental insulin resistance. J. Clin. Investig. **111:**1423–1432.

12. **Defronzo, R. A., R. C. Bonadonna, and E. Ferrannini.** 1992. Pathogenesis of NIDDM. A balanced overview. Diabetes Care **15:**318–368.

13. **Delibegovic, M., C. G. Armstrong, L. Dobbie, P. W. Watt, A. J. Smith, and P. T. Cohen.** 2003. Disruption of the striated muscle glycogen targeting subunit PPP1R3A of protein phosphatase 1 leads to increased weight gain, fat deposition, and development of insulin resistance. Diabetes **52:**596–604.

14. **Fang, X., S. X. Yu, Y. Lu, R. C. Bast, Jr., J. R. Woodgett, and G. B. Mills.** 2000. Phosphorylation and inactivation of glycogen synthase kinase 3 by protein kinase A. Proc. Natl. Acad. Sci. USA **97:**11960–11965.

15. **Filippa, N., C. L. Sable, C. Filloux, B. Hemmings, and E. Van Obberghen.** 1999. Mechanism of protein kinase B activation by cyclic AMP-dependent protein kinase. Mol. Cell. Biol. **19:**4989–5000.

16. **Guertin, D. A., D. M. Stevens, C. C. Thoreen, A. A. Burds, N. Y. Kalaany, J. Moffat, M. Brown, K. J. Fitzgerald, and D. M. Sabatini.** 2006. Ablation in mice of the mTORC components raptor, rictor, or mLST8 reveals that mTORC2 is required for signaling to Akt-FOXO and PKCalpha, but not S6K1. Dev. Cell **11:**859–871.

17. **Hara, K., Y. Maruki, X. Long, K. Yoshino, N. Oshiro, S. Hidayat, C. Tokunaga, J. Avruch, and K. Yonezawa.** 2002. Raptor, a binding partner of target of rapamycin (TOR), mediates TOR action. Cell **110:**177–189.

18. **He, A., X. Liu, L. Liu, Y. Chang, and F. Fang.** 2007. How many signals impinge on GLUT4 activation by insulin? Cell. Signal. **19:**1–7.

19. **Hori, H., T. Sasaoka, H. Ishihara, T. Wada, S. Murakami, M. Ishiki, and M. Kobayashi.** 2002. Association of SH2-containing inositol phosphatase 2 with the insulin resistance of diabetic db/db mice. Diabetes **51:**2387–2394.

20. **Hresko, R. C., and M. Mueckler.** 2005. mTOR. RICTOR is the Ser473 kinase for Akt/protein kinase B in 3T3-L1 adipocytes. J. Biol. Chem. **280:**40406–40416.

21. **Huang, S., and M. P. Czech.** 2007. The GLUT4 glucose transporter. Cell Metab. **5:**237–252.

22. **Inoki, K., Y. Li, T. Zhu, J. Wu, and K. L. Guan.** 2002. TSC2 is phosphorylated and inhibited by Akt and suppresses mTOR signalling. Nat. Cell Biol. **4:**648–657.

23. **Jacinto, E., V. Facchinetti, D. Liu, N. Soto, S. Wei, S. Y. Jung, Q. Huang, J. Qin, and B. Su.** 2006. SIN1/MIP1 maintains rictor-mTOR complex integrity and regulates Akt phosphorylation and substrate specificity. Cell **127:**125–137.

24. **Jacinto, E., R. Loewith, A. Schmidt, S. Lin, M. A. Ruegg, A. Hall, and M. N. Hall.** 2004. Mammalian TOR complex 2 controls the actin cytoskeleton and is rapamycin insensitive. Nat. Cell Biol. **6:**1122–1128.

25. **Kane, S., H. Sano, S. C. Liu, J. M. Asara, W. S. Lane, C. C. Garner, and G. E. Lienhard.** 2002. A method to identify serine kinase substrates. Akt phosphorylates a novel adipocyte protein with a Rab GTPase-activating protein (GAP) domain. J. Biol. Chem. **277:**22115–22118.

26. **Kim, Y. B., O. D. Peroni, W. G. Aschenbach, Y. Minokoshi, K. Kotani, A.**

Zisman, C. R. Kahn, L. J. Goodyear, and B. B. Kahn. 2005. Muscle-specific deletion of the Glut4 glucose transporter alters multiple regulatory steps in glycogen metabolism. Mol. Cell. Biol. 25:9713–9723.

27. Klip, A., and M. R. Paquet. 1990. Glucose transport and glucose transporters in muscle and their metabolic regulation. Diabetes Care 13:228–243.

28. Kohn, A. D., S. A. Summers, M. J. Birnbaum, and R. A. Roth. 1996. Expression of a constitutively active Akt Ser/Thr kinase in 3T3-L1 adipocytes stimulates glucose uptake and glucose transporter 4 translocation. J. Biol. Chem. 271:31372–31378.

29. Lawrence, J. C., Jr., J. F. Hiken, and D. E. James. 1990. Phosphorylation of the glucose transporter in rat adipocytes. Identification of the intracellular domain at the carboxyl terminus as a target for phosphorylation in intact-cells and in vitro. J. Biol. Chem. 265:2324–2332.

30. Lawrence, J. C., Jr., C. James, and J. F. Hiken. 1986. Control of glycogen synthase by insulin and isoproterenol in rat adipocytes. Changes in the distribution of phosphate in the synthase subunit in response to insulin and beta-adrenergic receptor activation. J. Biol. Chem. 261:669–677.

31. Manchester, J., A. V. Skurat, P. Roach, S. D. Hauschka, and J. C. Lawrence, Jr. 1996. Increased glycogen accumulation in transgenic mice overexpressing glycogen synthase in skeletal muscle. Proc. Natl. Acad. Sci. USA 93:10707–10711.

32. McManus, E. J., K. Sakamoto, L. J. Armit, L. Ronaldson, N. Shpiro, R. Marquez, and D. R. Alessi. 2005. Role that phosphorylation of GSK3 plays in insulin and Wnt signalling defined by knockin analysis. EMBO J. 24:1571–1583.

33. Michael, M. D., R. N. Kulkarni, C. Postic, S. F. Previs, G. I. Shulman, M. A. Magnuson, and C. R. Kahn. 2000. Loss of insulin signaling in hepatocytes leads to severe insulin resistance and progressive hepatic dysfunction. Mol. Cell 6:87–97.

34. Park, I. K., and A. A. DePaoli-Roach. 1994. Domains of phosphatase inhibitor-2 involved in the control of the ATP-Mg-dependent protein phosphatase. J. Biol. Chem. 269:28919–28928.

35. Parker, P. J., F. B. Caudwell, and P. Cohen. 1983. Glycogen synthase from rabbit skeletal muscle; effect of insulin on the state of phosphorylation of the seven phosphoserine residues in vivo. Eur. J. Biochem. 130:227–234.

36. Passonneau, J. V., and V. R. Lauderdale. 1974. A comparison of three methods of glycogen measurement in tissues. Anal. Biochem. 60:405–412.

37. Pederson, B. A., J. M. Schroeder, G. E. Parker, M. W. Smith, A. A. DePaoli-Roach, and P. J. Roach. 2005. Glucose metabolism in mice lacking muscle glycogen synthase. Diabetes 54:3466–3473.

38. Roach, P. J. 2002. Glycogen and its metabolism. Curr. Mol. Med. 2:101–120.

39. Rylatt, D. B., A. Aitken, T. Bilham, G. D. Condon, N. Embi, and P. Cohen. 1980. Glycogen synthase from rabbit skeletal muscle. Amino acid sequence at the sites phosphorylated by glycogen synthase kinase-3, and extension of the N-terminal sequence containing the site phosphorylated by phosphorylase kinase. Eur. J. Biochem. 107:529–537.

40. Ryves, W. J., L. Fryer, T. Dale, and A. J. Harwood. 1998. An assay for glycogen synthase kinase 3 (GSK-3) for use in crude cell extracts. Anal. Biochem. 264:124–127.

41. Sakamoto, K., M. F. Hirshman, W. G. Aschenbach, and L. J. Goodyear. 2002. Contraction regulation of Akt in rat skeletal muscle. J. Biol. Chem. 277:11910–11917.

42. Sano, H., S. Kane, E. Sano, C. P. Miinea, J. M. Asara, W. S. Lane, C. W. Garner, and G. E. Lienhard. 2003. Insulin-stimulated phosphorylation of a Rab GTPase-activating protein regulates GLUT4 translocation. J. Biol. Chem. 278:14599–14602.

43. Sarbassov, D. D., S. M. Ali, D. H. Kim, D. A. Guertin, R. R. Latek, H. Erdjument-Bromage, P. Tempst, and D. M. Sabatini. 2004. Rictor, a novel binding partner of mTOR, defines a rapamycin-insensitive and raptor-independent pathway that regulates the cytoskeleton. Curr. Biol. 14:1296–1302.

44. Sarbassov, D. D., D. A. Guertin, S. M. Ali, and D. M. Sabatini. 2005. Phosphorylation and regulation of Akt/PKB by the rictor-mTOR complex. Science 307:1098–1101.

45. Scott, P. H., G. J. Brunn, A. D. Kohn, R. A. Roth, and J. C. Lawrence, Jr. 1998. Evidence of insulin-stimulated phosphorylation and activation of the mammalian target of rapamycin mediated by a protein kinase B signaling pathway. Proc. Natl. Acad. Sci. USA 95:7772–7777.

46. Scott, P. H., and J. C. Lawrence, Jr. 1998. Attenuation of mammalian target of rapamycin activity by increased cAMP in 3T3-L1 adipocytes. J. Biol. Chem. 273:34496–34501.

47. Scrimgeour, A. G., P. B. Allen, A. A. Fienberg, P. Greengard, and J. C. Lawrence, Jr. 1999. Inhibitor-1 is not required for the activation of glycogen synthase by insulin in skeletal muscle. J. Biol. Chem. 274:20949–20952.

48. Shiota, C., J. T. Woo, J. Lindner, K. D. Shelton, and M. A. Magnuson. 2006. Multiallelic disruption of the rictor gene in mice reveals that mTOR complex 2 is essential for fetal growth and viability. Dev. Cell 11:583–589.

49. Shulman, G. I., D. L. Rothman, T. Jue, P. Stein, R. A. Defronzo, and R. G. Shulman. 1990. Quantitation of muscle glycogen synthesis in normal subjects and subjects with non-insulin-dependent diabetes by 13C nuclear magnetic resonance spectroscopy. N. Engl. J. Med. 322:223–228.

50. Sutherland, C., and P. Cohen. 1994. The alpha-isoform of glycogen synthase kinase-3 from rabbit skeletal muscle is inactivated by p70 S6 kinase or MAP kinase-activated protein kinase-1 in vitro. FEBS Lett. 338:37–42.

51. Suzuki, Y., C. Lanner, J. H. Kim, P. G. Vilardo, H. Zhang, J. Yang, L. D. Cooper, M. Steele, A. Kennedy, C. B. Bock, A. Scrimgeour, J. C. Lawrence, Jr., and A. A. DePaoli-Roach. 2001. Insulin control of glycogen metabolism in knockout mice lacking the muscle-specific protein phosphatase PP1G/RGL. Mol. Cell. Biol. 21:2683–2694.

52. Thomas, J. A., K. K. Schlender, and J. Larner. 1968. A rapid filter paper assay for UDPglucose-glycogen glucosyltransferase, including an improved biosynthesis of UDP-14C-glucose. Anal. Biochem. 25:486–499.

53. Vander Haar, E., S. I. Lee, S. Bandhakavi, T. J. Griffin, and D. H. Kim. 2007. Insulin signalling to mTOR mediated by the Akt/PKB substrate PRAS40. Nat. Cell Biol. 9:316–323.

54. Whiteman, E. L., H. Cho, and M. J. Birnbaum. 2002. Role of Akt/protein kinase B in metabolism. Trends Endocrinol. Metab. 13:444–451.

55. Wullschleger, S., R. Loewith, and M. N. Hall. 2006. TOR signaling in growth and metabolism. Cell 124:471–484.

56. Yoshizaki, T., T. Imamura, J. L. Babendure, J. C. Lu, N. Sonoda, and J. M. Olefsky. 2007. Myosin 5a is an insulin-stimulated Akt2 (protein kinase Bβ) substrate modulating GLUT4 vesicle translocation. Mol. Cell. Biol. 27:5172–5183.

57. Zisman, A., O. D. Peroni, E. D. Abel, M. D. Michael, F. Mauvais-Jarvis, B. B. Lowell, J. F. Wojtaszewski, M. F. Hirshman, A. Virkamaki, L. J. Goodyear, C. R. Kahn, and B. B. Kahn. 2000. Targeted disruption of the glucose transporter 4 selectively in muscle causes insulin resistance and glucose intolerance. Nat. Med. 6:924–928.